

Power Quality Analysis of Six Phase Indirect Matrix Converter Based on Multi Phase Generator

Chabi S. SANNI^{1,3}, Augustin MPANDA MABWE² and Ahmed El HAJJAJI¹

¹Laboratoire MIS, UPJV

33 rue Saint Leu, 80039 Amiens, France

e-mail : salomon.sanni@unilasalle.fr, ahmed.hajjaji@u-picardie.fr

²SYMADE, UniLaSalle Amiens

14 Quai de la Somme, 80082 Amiens France

e-mail : augustin.mpanda@unilasalle.fr

³ADEME 20, avenue du Grésillé- BP 90406 49004 Angers Cedex 01 France

Abstract. Nowadays, multiphase machine drives are considered in many applications, especially for medium and high-power applications. This paper focuses on the topology of the six to three phase (hexaphase) indirect matrix converter (IMC). The matrix converter (MC) is designed based on twelve bidirectional switches for the rectifier stage and six single switches for the inverter stage. It is interfaced to a high-performance, fault-tolerant multiphase permanent magnet synchronous generator (PMSG) on one side and to the grid on the other side. In the literature, the most common MCs are of the three-phase type and papers on multiple input converters ($N>3$) are not common. This paper deals with all possible configurations of SVM that can be deduced in a hexaphase MC to determine the modulation indexes and then to assess the VTR (Voltage Transfer Ratio). Simulations are performed on a pure inductive load and THD analysis are performed on the input currents of the MC to show the impact of the studied configurations on the system.

Key words. Indirect Matrix Converter (IMC), Direct Matrix Converter (DMC), Space Vector Modulation (SVM), Synchronous generator, Voltage Transfer Ratio (VTR)

1. Introduction

For many decades, considerable attention has been devoted to power electronic converters highlighting their major types, basic principles of operation, key applications, and distinctive feature. The MC has got such attention, especially at the generation level as it replaces the classic back-to-back (B2B) converter while offering many advantages such as sinusoidal (input/output) currents, a unitary power factor besides being more compact and offering a longer life duration due to the absence of passive elements such as capacitors.

There are two types of MC, the conventional also called direct configuration (DMC) and the indirect configuration (IMC). The MC is used in applications such as engine controls, wind energy conversion systems (WECS), electrical systems for aeronautics and variable speed diesel generation systems. Several publications on the indirect modulation technique of $3\Phi - 3\Phi$ MC are available and refer to the Space Vector Modulation (SVM) whose maximum

voltage transfer ratio (VTR) is 86%. So, it works as a step-down voltage [1]–[5].

Generally, in the development of the SVM the rectifier and inverter stages are synchronized to obtain the duty cycles of the switches. In [2], these two stages are controlled separately. The efficiency of the studied system is around 92% and no VTR is provided.

The multiphase machines ($N>3$) offer, among other intrinsic advantages, high unit power, high fault tolerance, greater reliability, and low torque ripple rate. However, these machines require new converter structures to be interfaced to the grid. Several studies [6–10] have been carried out on the improvement of the VTR and the overall efficiency of MCs. In the literature, few papers deal with the use of SVM on MCs applied to polyphase systems of type $3\Phi - N\Phi$. For a $3\Phi - 5\Phi$ system the VTR is 78.86% [6]–[10] and 76.93% for a $3\Phi - 7\Phi$ system [11]. For a $3\Phi - 9\Phi$ system a minimum VTR of 76% and maximum of 94.5% is reported in [12]. However, very few papers deal with $N\Phi - 3\Phi$ systems with MCs. Paper [13] is a previous work of our team on a $6\Phi - 3\Phi$ hexaphase MC applied to a DMC connected to the network. This paper uses only the largest amplitude active vectors of the rectifier complex plane for the SVM.

The article [14] develops the SVM for a $5\Phi - 3\Phi$ system for a DMC using the direct SVM approach as well as the carrier-based technique. This article does not give the VTR for this system. Nevertheless, the paper [15] proposes an SVM whose results allow to have a VTR of 104.4%, which is really an improvement as it allows the MC to operate in boost mode.

In this project, the system under study is a $6\Phi - 3\Phi$ hexaphase matrix converter as shown in Fig. 1 applied to an IMC connected to the grid. All the rectifier and inverter stages are controlled using the indirect SVM modulation technique. Due to space limitation, this paper presents the possible configurations that may be deduced with the hexaphase IMC structure. Then, the modulation indexes of the rectifier and the inverter stages can be determined and therefore, the VTR assessed. The SVM modulation technique will be presented in future publication.

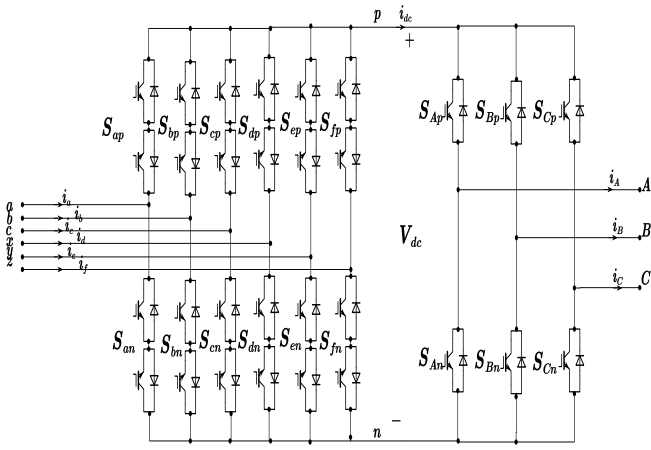


Fig. 1. Complete configuration of the hexaphase IMC

2. SVM technique for 6Φ-3Φ IMC

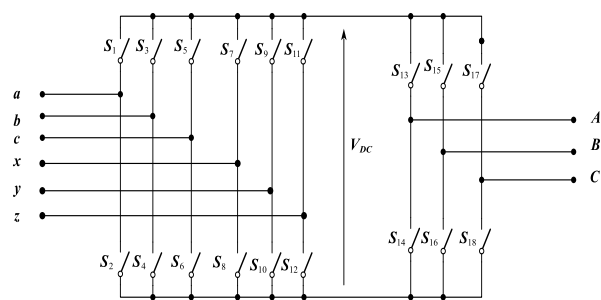


Fig. 2. Illustrative diagram of the hexaphase IMC

The 6Φ-3Φ indirect matrix converter has twelve bidirectional switches for the rectifier stage and six single switches for the inverter stage. The input voltage and current vectors are given by the following expressions:

$$\begin{cases} \mathbf{V}_{in} = \left(\frac{1}{3}\right) \left(\mathbf{V}_a + \mathbf{V}_b e^{j\frac{2\pi}{3}} + \mathbf{V}_c e^{j\frac{4\pi}{3}} + \mathbf{V}_x e^{j\frac{\pi}{6}} + \mathbf{V}_y e^{j\frac{5\pi}{6}} + \mathbf{V}_z e^{j\frac{3\pi}{2}} \right) \\ \mathbf{I}_{in} = \left(\frac{1}{3}\right) \left(\mathbf{I}_a + \mathbf{I}_b e^{j\frac{2\pi}{3}} + \mathbf{I}_c e^{j\frac{4\pi}{3}} + \mathbf{I}_x e^{j\frac{\pi}{6}} + \mathbf{I}_y e^{j\frac{5\pi}{6}} + \mathbf{I}_z e^{j\frac{3\pi}{2}} \right) \end{cases} \quad (1)$$

The analytical expressions for the output voltage and current vectors are of the following form:

$$\begin{cases} \mathbf{V}_{out} = \left(\frac{2}{3}\right) \left(\mathbf{V}_A + \mathbf{V}_B e^{j\frac{2\pi}{3}} + \mathbf{V}_C e^{j\frac{4\pi}{3}} \right) \\ \mathbf{I}_{out} = \left(\frac{2}{3}\right) \left(\mathbf{I}_A + \mathbf{I}_B e^{j\frac{2\pi}{3}} + \mathbf{I}_C e^{j\frac{4\pi}{3}} \right) \end{cases} \quad (2)$$

A. Active vectors and vector plane of the inverter stage

The inverter stage is connected to an inductive load. By considering the interconnection laws of the energy sources, the output phases must not be open circuit. Then, the number of possible combinations of interconnections of phases is eight (2^3) with six active vectors and two zero vectors as shown in Table I. The complex plane is defined by the hexagon below (Fig. 3).

Table I. Table of inverter stage switch combinations

A	B	C	Module	Angle (rad)
0	0	0	0	-
0	0	1	$(2/3)V_{DC}$	$-2\pi/3$
0	1	0	$(2/3)V_{DC}$	$2\pi/3$
0	1	1	$(2/3)V_{DC}$	π
1	0	0	$(2/3)V_{DC}$	0
1	0	1	$(2/3)V_{DC}$	$-\pi/3$
1	1	0	$(2/3)V_{DC}$	$\pi/3$
1	1	1	0	-

The SVM of the inverter stage is based on the output vectors which are expressed in (3) and (4).

$$\begin{bmatrix} \mathbf{V}_A \\ \mathbf{V}_B \\ \mathbf{V}_C \end{bmatrix} = \begin{bmatrix} S_{13} & S_{14} \\ S_{15} & S_{16} \\ S_{17} & S_{18} \end{bmatrix} * \begin{bmatrix} \mathbf{V}_{DC+} \\ \mathbf{V}_{DC-} \end{bmatrix} \quad (3)$$

$$\begin{bmatrix} \mathbf{I}_{DC+} \\ \mathbf{I}_{DC-} \end{bmatrix} = \begin{bmatrix} S_{13} & S_{15} & S_{17} \\ S_{14} & S_{16} & S_{18} \end{bmatrix} * \begin{bmatrix} \mathbf{I}_A \\ \mathbf{I}_B \\ \mathbf{I}_C \end{bmatrix} \quad (4)$$

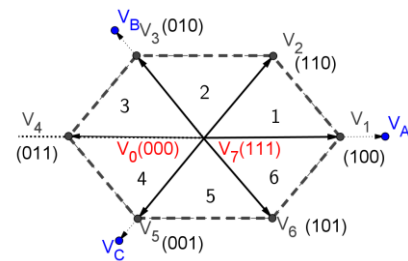


Fig. 3. Complex plan of the inverter stage

B. Active vectors and vector plane of the rectifier stage

The rectifier stage is supplied by a voltage source. By considering the interconnection laws of the energy sources, the input phases must not be short-circuited. Then, the number of available combinations of interconnections of phases is thirty-six (6^2), thirty active vectors and six null vectors as figured in Table II. The complex plane is defined by Fig. 4 and Fig. 5.

The rectifier stage SVM is based on the input vectors as follow:

$$\begin{bmatrix} \mathbf{I}_a \\ \mathbf{I}_b \\ \mathbf{I}_c \\ \mathbf{I}_x \\ \mathbf{I}_y \\ \mathbf{I}_z \end{bmatrix} = \begin{bmatrix} S_1 & S_2 \\ S_3 & S_4 \\ S_5 & S_6 \\ S_7 & S_8 \\ S_9 & S_{10} \\ S_{11} & S_{12} \end{bmatrix} * \begin{bmatrix} \mathbf{I}_{DC+} \\ \mathbf{I}_{DC-} \end{bmatrix} \quad (5)$$

$$\begin{bmatrix} \mathbf{V}_{DC+} \\ \mathbf{V}_{DC-} \end{bmatrix} = \begin{bmatrix} S_1 & S_3 & S_5 & S_7 & S_9 & S_{11} \\ S_2 & S_4 & S_6 & S_8 & S_{10} & S_{12} \end{bmatrix} * \begin{bmatrix} \mathbf{V}_a \\ \mathbf{V}_b \\ \mathbf{V}_c \\ \mathbf{V}_x \\ \mathbf{V}_y \\ \mathbf{V}_z \end{bmatrix} \quad (6)$$

Table II. Table of rectifier stage switch combinations

	a	b	c	x	y	z
a		ab	ac	ax	ay	az
b	ba		bc	bx	by	bz
c	ca	cb		cx	cy	cz
x	xa	xb	xc		xy	xz
y	ya	yb	yc	yx		yz
z	za	zb	zc	zx	zy	

Table III. Table of active vectors of the rectifier stage

	Module	Angle(°)		Module	Angle(°)
ab	0.5774	-30	xa	0.1725	105
ac	0.5774	30	xb	0.4714	-15
ad	0.1725	-75	xc	0.6440	45
ay	0.6440	-15	xy	0.5774	0
az	0.4714	45	xz	0.5774	60
ba	0.5774	150	ya	0.6440	165
bc	0.5774	90	yb	0.1725	-135
bx	0.4714	165	yc	0.4714	105
by	0.1725	45	yx	0.5774	180
bz	0.6440	105	yz	0.5774	120
ca	0.5774	-150	za	0.4714	-135
cb	0.5774	-90	zb	0.6440	-75
cx	0.6440	-135	zc	0.1725	-15
cy	0.4714	-75	zx	0.5774	-120
cz	0.1725	165	zy	0.5774	-60

Thanks to the above table, two complex planes can be defined for the SVM control. The first one is composed by the active vectors colored in yellow and the second plane has its active vectors colored in white, green and blue.

With these two complex plans, three configurations are defined for the development of the SVM control.

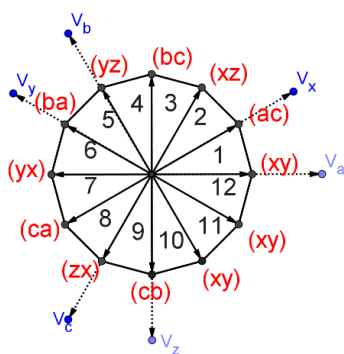


Fig. 4. VSR first complex plane (12 active vectors)

Do_vectors (Scheme1): Use of the 12 active vectors of the Dodecagon for the control with the magnitude of $|D|=0.5774V_{dc}$.

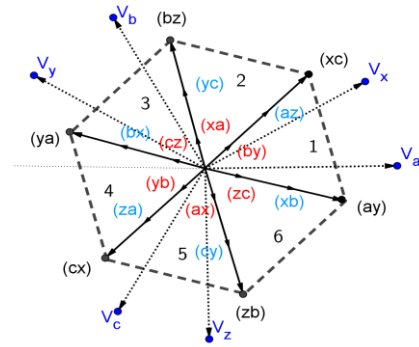


Fig. 5. VSR second complex plane (18 active vectors)

The hexagon with 18 active vectors leads to 3 main groups of active vector amplitudes which are: Large: $|L|=0.6440V_{dc}$, Medium: $|M|=0.4714V_{dc}$ and Small: $|S|=0.1725V_{dc}$.

Sx_vectors (Scheme2): Use of the six large active vectors

Tw_vectors (Scheme3): Use of the six large and six medium actives vectors

3. Determination of the VTR for each of the three configurations

A. Do_vectors Configuration (Scheme1)

- 1) Determination of the modulation indexes of the rectifier stage (m_c) and the inverter stage (m_v)
 - a) Modulation index m_v

The projections of the sector reference voltage vector V^* on the α and β axes are given by the following complex expressions:

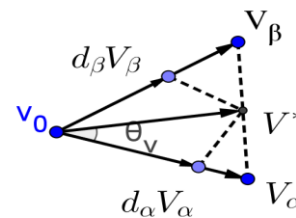


Fig. 6. VSI SVM vector sector

Using Fig.6,

$$VT_s = V_{ref} e^{j\theta} T_s$$

$$VT_s = V_\alpha T_\alpha + V_\beta T_\beta + V_0 T_0 \quad (7)$$

$T_s = T_\alpha + T_\beta + T_0$ and V_0 is the zero vector.

Assuming that sector 1 of Fig.4 is considered and according to Table I, (8) is obtained :

$$\begin{cases} V_\alpha(100) = \frac{2}{3} V_d \\ V_\beta(110) = \frac{2}{3} V_d e^{j\pi/3} \end{cases} \quad (8)$$

Then, from (7) and (8), it comes (9):

$$V_{ref} e^{j\theta} T_s = \frac{2}{3} V_d T_\alpha + \frac{2}{3} V_d e^{(j\pi/3)} T_\beta \quad (9)$$

After developing (9) and separating it in real and imaginary parts, it comes :

$$\begin{cases} V_{ref} \cos\theta T_s = \frac{2}{3} V_d T_\alpha + \frac{2}{3} V_d T_\beta \\ V_{ref} \sin\theta T_s = \frac{1}{\sqrt{3}} V_d T_\beta \end{cases} \quad (10)$$

The duty cycles of the vectors on the α and β axes are therefore given by:

$$\begin{cases} \frac{T_\alpha}{T_s} = \frac{\sqrt{3} V_{ref}}{V_d} \sin(\frac{\pi}{3} - \theta) \\ \frac{T_\beta}{T_s} = \frac{\sqrt{3} V_{ref}}{V_d} \sin(\theta) \end{cases} \quad (11)$$

From the equation (8), the modulation index m_v is as follows:

$$m_v = \frac{\sqrt{3} V_{ref}}{V_d} \quad (12)$$

b) Modulation index m_c

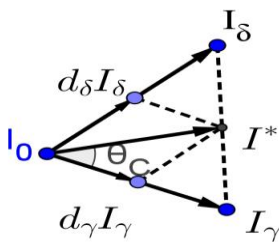


Fig. 7. VSR SVM vector sector scheme 1

From Fig. 7, the projections of the sector reference current vector I^* on the γ and δ axes lead to relationships in (13):

$$\begin{aligned} I T_s &= I_{ref} e^{j\theta} T_s \\ I T_s &= I_\gamma T_\gamma + I_\delta T_\delta + I_0 T_0 \\ T_s &= T_\gamma + T_\delta + T_0 \end{aligned} \quad (13)$$

With I_0 the zero vector. Considering sector 1 and according to Table III, the relationships in (14) are obtained.

$$\begin{cases} I_\gamma (ab) = 0.5774 I_d e^{(j\pi/6)} \\ I_\delta (xy) = 0.5774 I_d e^{(j0)} \end{cases} \quad (14)$$

From (13) and (14):

$$I_{ref} e^{j\theta} T_s = 0.5774 I_d e^{(j\pi/6)} T_\gamma + 0.5774 I_d e^{(j0)} T_\delta \quad (15)$$

After expanding (15) and separating it in real and imaginary parts (16) is obtained.

$$\begin{cases} I_{ref} \cos\theta T_s = 0.5774 I_d \left(\left(\frac{\sqrt{3}}{2} \right) T_\gamma + T_\delta \right) \\ I_{ref} \sin\theta T_s = \frac{1}{\sqrt{3}} I_d \left(-\frac{T_\gamma}{2} \right) \end{cases} \quad (16)$$

The duty cycles of the vectors on the γ and δ axes are defined as:

$$\begin{cases} \frac{T_\gamma}{T_s} = 3.464 \frac{I_{ref}}{I_d} \sin(\pi + \theta) \\ \frac{T_\delta}{T_s} = 3.464 \frac{I_{ref}}{I_d} \sin\left(\frac{\pi}{6} + \theta\right) \end{cases} \quad (17)$$

From the equation (17), the deduced modulation index m_c is then expressed as in (18):

$$m_c = 3.464 \frac{I_{ref}}{I_d} \quad (18)$$

2) VTR calculation (q_{max})

The VTR, maximum voltage transfer ratio, is the quotient of the output voltage of the converter on its input voltage.

$$q_{max} = \left(\frac{V_{out_{max}}}{V_{in}} \right) \quad (19)$$

Assumption:

For an optimum power transfer, it is assumed that there is no power loss within the DC bus. The considered powers are then expressed as:

Hexaphase Input Power	$P_{in} = 3 V_{in} I_{in} \cos\phi$
DC Bus Power	$P_{DC} = V_d I_d$
Triphase output Power	$P_{out} = \frac{3}{2} V_{out} I_{out} \cos\phi$

a) Relationship between the input voltage and the DC bus voltage

The assumption above leads to:

$$\begin{aligned} P_{DC} &= P_{in} \\ V_d I_d &= 3 V_{in} I_{in} \cos\phi \end{aligned}$$

Then, expanding the above equation and introducing the current modulation index leads to (20).

$$V_d = \frac{\sqrt{3}}{2} V_{in} m_c \cos\phi \quad (20)$$

For $m_c=1$ and at unit power factor, the relation between the input voltage and the DC bus voltage is expressed as:

$$V_d = \frac{\sqrt{3}}{2} V_{in} \quad (21)$$

b) Relationship between the output current and the DC bus current

Considering the same assumption about the equality of input, output and DC Bus powers, the DC current is then expressed as a function of voltage modulation index.

$$I_d = \frac{\sqrt{3}}{2} I_{out} m_v \cos\phi \quad (22)$$

For $m_v=1$ and a unit power factor, the relationship between the output current and the DC bus current is as follows:

$$I_{out} = \frac{2}{\sqrt{3}} I_d \quad (23)$$

c) Relationship between the output voltage and the DC bus voltage

Considering $P_{DC}=P_{out}$, I_{out} given by (23) and unity power factor, the relationship between the output voltage and the DC bus voltage is obtained as:

$$V_d = \sqrt{3} V_{out} \quad (24)$$

Using (21), (23) and (24) the VTR is calculated as follow:

$$q_{max} = \frac{V_{out_{max}}}{V_d} \frac{V_d}{V_{in}} \quad (25)$$

$$q_{max} = \frac{1}{2} \quad (26)$$

The VTR of Do_vectors configuration is 50% of the input voltage.

For the rest of the calculations, the expression of the inverter stage modulation index is maintained as in (12).

B. Sx_vectors Configuration (Scheme2)

1) Determination of the rectifier stage modulation index (m_c)

The complex expressions for the projections of the reference current vector of the sector on the γ and δ axes are the same as those in (13).

Considering the sector 1 and according to Table III, it comes :

$$\begin{cases} I_\gamma (ay) = 0.644 I_d e^{-j\pi/12} \\ I_\delta (xc) = 0.644 I_d e^{j\pi/4} \end{cases} \quad (27)$$

From (13) and (27) similarly to (15):

$$I_{ref} e^{j0} T_s = 0.644 I_d e^{(j\pi/6)} T_\gamma + 0.644 I_d e^{(j0)} T_\delta \quad (28)$$

The expansion of (28) and its separation in real and imaginary parts yields to (29):

$$\begin{cases} I_{ref} \cos\theta T_s = I_d ((0.62203 T_\gamma + 0.45537 T_\delta)) \\ I_{ref} \sin\theta T_s = I_d (0.45537 T_\delta - 0.1667 T_\gamma) \end{cases} \quad (29)$$

The duty cycles of the vectors on the γ and δ axes are defined as:

$$\begin{cases} \frac{T_\gamma}{T_s} = 1.793 \frac{I_{ref}}{I_d} \sin(\frac{\pi}{12} + \theta) \\ \frac{T_\delta}{T_s} = 1.793 \frac{I_{ref}}{I_d} \sin(\frac{\pi}{4} - \theta) \end{cases} \quad (30)$$

From (30), the modulation index m_c is deduced as follows:

$$m_c = 1.793 \frac{I_{ref}}{I_d} \quad (31)$$

2) VTR calculation (q_{max})

The steps used to determine the following relationships are the same as those used for the Do_vectors configuration.

a) The link between the input voltage and the DC bus voltage

$$V_d = 1.673 V_{in} \quad (32)$$

b) The link between the output current and the DC bus current

$$I_{out} = \frac{2}{\sqrt{3}} I_d \quad (33)$$

c) The link between the output voltage and the DC bus voltage

$$V_d = \sqrt{3} V_{out} \quad (34)$$

Using (32), (33) and (34) the VTR is calculated as in (25) leading to $q_{max}=0.966$ which means that the VTR of Sx_vectors configuration is 96.6% of the input voltage.

C. Tw_vectors Configuration (Scheme3)

1) Determination of the rectifier stage modulation index (m_c)

In this configuration, four active vectors in each sector are considered which give two components of the sector's reference current vector on the γ and the δ axes. The order in which the active vectors are treated is of importance and it is given as follows $I_0, I'_\gamma, I''_\delta, I''_\gamma, I'_\delta$ and I_0 :

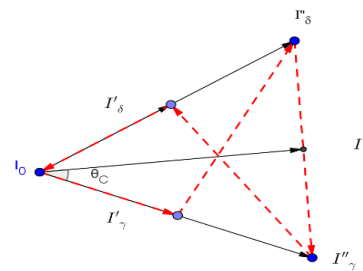


Fig. 8. VSR SVM vector sector scheme 3

The reference current vector expression is given by (35).

$$I T_s = I'_\gamma T'_\gamma + I''_\delta T''_\delta + I''_\gamma T''_\gamma + I'_\delta T'_\delta + I_0 T_0 = I e^{j0} T_s \quad (35)$$

Given that :

$$\begin{cases} T_\gamma = T'_\gamma + T''_\delta \\ T_\delta = T''_\gamma + T'_\delta \end{cases} \quad (36)$$

$T_s = T_\gamma + T_\delta + T_0$ and I_0 is the zero vector.

The duty cycles of the medium and the larger vectors are evaluated below.

a) *Medium* vectors

$$I \cdot T'_s = I_\gamma T'_\gamma + I_\delta T'_\delta + I_0 T_0 = I e^{j\theta} T'_s \quad (37)$$

$T'_s = T'_\gamma + T'_\delta + T_0$ and I_0 is the zero vector.

Assuming that sector 1 is considered and according to Table III, (38) and (39) are obtained:

$$\begin{cases} I'_\gamma(xb) = 0.4714 I_d e^{j\frac{\pi}{12}} \\ I'_\delta(az) = 0.4714 I_d e^{j\frac{\pi}{4}} \end{cases} \quad (38)$$

$$I_{ref} e^{j\theta} T'_s = 0.4714 I_d e^{j\left(\frac{\pi}{12}\right)} T'_\gamma + 0.4714 I_d e^{j\left(\frac{\pi}{4}\right)} T'_\delta \quad (39)$$

Expanding and separating in real and imaginary parts the above equation lead to (40):

$$\begin{cases} I_{ref} \cos\theta T'_s = I_d (0.455 T'_\gamma + 0.3333 T'_\delta) \\ I_{ref} \sin\theta T'_s = \frac{1}{\sqrt{3}} I_d (0.3333 T'_\delta - 0.122 T'_\gamma) \end{cases} \quad (40)$$

The duty cycles of the vectors on the γ and δ axes are defined as:

$$\begin{cases} \frac{T'_\gamma}{T'_s} = 2.45 \frac{I_{ref}}{I_d} \sin\left(\frac{\pi}{4} - \theta\right) \\ \frac{T'_\delta}{T'_s} = 2.45 \frac{I_{ref}}{I_d} \sin\left(\frac{\pi}{12} + \theta\right) \end{cases} \quad (41)$$

From the equation (41), the modulation index m'_c is deduced as follows:

$$m'_c = 2.45 \frac{I_{ref}}{I_d} \quad (42)$$

b) - *Larger* vectors

The approach for determining the duty cycles of the vectors is the same as for the medium vectors. The duty cycles of the vectors on the γ and δ axes are defined as:

$$\begin{cases} \frac{T''_\gamma}{T''_s} = 1.793 \frac{I_{ref}}{I_d} \sin\left(\frac{\pi}{12} + \theta\right) \\ \frac{T''_\delta}{T''_s} = 1.793 \frac{I_{ref}}{I_d} \sin\left(\frac{\pi}{4} - \theta\right) \end{cases} \quad (43)$$

From the equation (43), the modulation index is then:

$$m''_c = 1.793 \frac{I_{ref}}{I_d} \quad (44)$$

- For the global configuration

$$\begin{aligned} T_\gamma &= T'_\gamma + T''_\delta \\ T_\delta &= T''_\gamma + T'_\delta \end{aligned} \quad (45)$$

The duty cycles of the global vectors on the γ and δ axes:

$$\begin{cases} \frac{T_\gamma}{T_s} = 2.196 \frac{I_{ref}}{I_d} \sin\left(\frac{\pi}{3} + \theta\right) \\ \frac{T_\delta}{T_s} = 2.196 \frac{I_{ref}}{I_d} \sin\left(\frac{\pi}{2} + \theta\right) \end{cases} \quad (46)$$

From the equation (46), the modulation index for the global configuration is then obtained:

$$m_c = 2.196 \frac{I_{ref}}{I_d} \quad (47)$$

2) *VTR calculation* (q_{max})

The steps used to determine the following relationships are the same as those used for the Do_vectors configuration.

c) *The link between the input voltage and the DC bus voltage*

$$V_d = 1.366 V_{in} \quad (48)$$

d) *The link between the output current and the DC bus current*

$$I_{out} = \frac{2}{\sqrt{3}} I_d \quad (49)$$

e) *The link between the output voltage and the DC bus voltage*

$$V_d = \sqrt{3} V_{out} \quad (50)$$

Using (50), (51) and (52) the VTR is calculated:

$$q_{max} = \frac{V_{out,max}}{V_d} \frac{V_d}{V_{in}} \quad (51)$$

$$q_{max} = 0.789 \quad (52)$$

The VTR of Tw_vectors configuration is 78.9% of the input voltage.

Table IV. Summary of theoretical configurations studied.

Config uration	3 ϕ -3 ϕ	6 ϕ -3 ϕ Do_vectors (Scheme 1)	6 ϕ -3 ϕ Sx_vectors (Scheme2)	6 ϕ -3 ϕ Tw_vector s (Scheme3)
VTR (%)	86.6	50	96.6	78.9
m_c	$\frac{I_{ref}}{I_d}$	$3.464 \frac{I_{ref}}{I_d}$	$1.793 \frac{I_{ref}}{I_d}$	$m_c = 2.196 \frac{I_{ref}}{I_d}$ $m'_c = 2.45 \frac{I_{ref}}{I_d}$ $m''_c = 1.793 \frac{I_{ref}}{I_d}$
m_v	$\sqrt{3} * \frac{V_{ref}}{V_d}$			

4. SIMULATION RESULTS

The SVM modulation technique is developed for the configuration of scheme 2 and scheme 3. The scheme 1 is not considered as the evaluated VTR is too low. Simulations in closed-loop according to the system represented in Fig.9 with a 3 ϕ -3 ϕ and a 6 ϕ -3 ϕ IMC are performed on a RL-load.

Below are given the THDs of the input currents and output voltages for 3 systems considered, 3 ϕ -3 ϕ , 6 ϕ -3 ϕ with scheme2 and 6 ϕ -3 ϕ with scheme3.

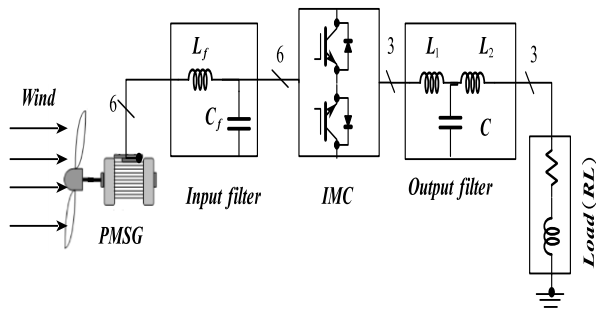


Fig. 9. System overview scheme without control part

Table V. Simulation parameters

PMSG	Power rating	1.5MVA
	Wind speed	11m/s
Load	$R = 0.463\Omega; L = 713.37\mu H$	

Table VI. Simulation results for all configurations

	3 ϕ -3 ϕ		6 ϕ -3 ϕ Sx_vectors (Scheme2)		6 ϕ -3 ϕ Tw_vectors (Scheme3)	
	Max values	THD (%)	Max values	THD (%)	Max values	THD (%)
V_{PMSG} (V)	834.7	0.02	742.3	0.09	742.3	0.09
I_{PMSG} (A)	1049	0.29	558.6	41.59	404.8	7.79
$V_{in,MC}$ (V)	832.1	1.13	733.2	6.45	738.3	2.26
$I_{in,MC}$ (A)	1041	64	545.4	106.7	388.4	138
$V_{out,MC}$ (V)	719.8	75.55	691.3	80.10	565.9	87.32
V_{load} (V)	687.7	1.11	645.1	2.12	540.2	0.65
I_{load} (A)	1337	0.07	1254	0.92	1050	0.11
VTR (%)	86.5		95.4		76.6	

Considering the input and output voltages directly measured on the MC, the VTR evaluated in all configurations are close to theoretical values in table IV.

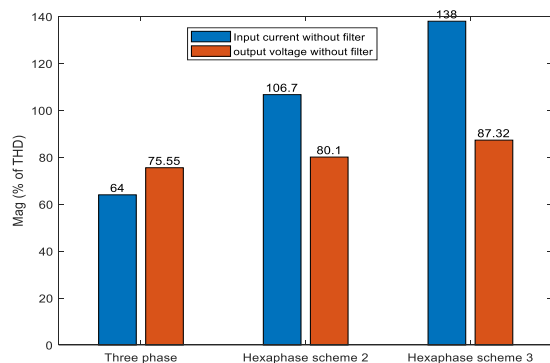


Fig. 10. THD of the input current (PMSG) and load voltage without filter

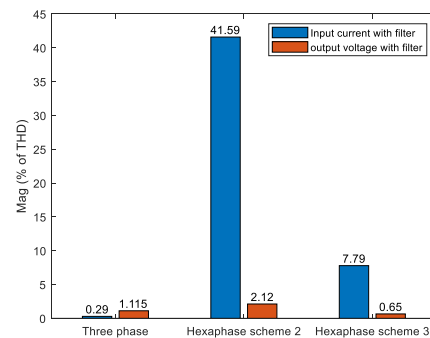


Fig. 11. THD of the input current (PMSG) and load voltage with filter

5. Conclusion

The purpose of this paper is to study all possible configuration schemes and determine the maximum associated voltage transfer ratio (VTR). Table IV summarizes all the possible configurations. The highest VTR (96.6%) comes with the hexaphase system which is higher than the three-phase VTR (86.6%), and the minimum is 50%. The Sx_vectors configuration (96.6% VTR) has a higher THD due to the presence of rank 3 harmonics. It can be observed that the higher the number of active vectors used (Tw_vectors configuration), the lower the THD. The reason is because the rank 3 harmonics are lower with less switching losses.

A logical follow-up to this publication is the development of the SVM modulation technique to be published soon.

Acknowledgment

This work was supported by the French Environment and Energy Management Agency (ADEME) and the Hauts de France Region.

References

- [1] L. Huber et D. Borojovic, « Space vector modulated three-phase to three-phase matrix converter with input power factor correction », IEEE Trans. Ind. Appl., vol. 31, no 6, p. 1234-1246, déc. 1995, doi: 10.1109/28.475693.
- [2] O. R. Saiyappa et N. S. Kumar, « An Indirect Space Vector Scheme for IMC applied to PMSG based Wind Energy Conversion Systems », in 2019 Fifth International Conference on Electrical Energy Systems (ICEES), Chennai, India: IEEE, févr. 2019, p. 1-7. doi: 10.1109/ICEES.2019.8719311.
- [3] D. Varajão et R. E. Araújo, « Modulation Methods for Direct and Indirect Matrix Converters: A Review », Electronics, vol. 10, no 7, p. 812, mars 2021, doi: 10.3390/electronics10070812.
- [4] Z. Malekjamshidi, M. Jafari, D. Xiao, et J. Zhu, « Operation of indirect matrix converters in different SVM switching patterns », in 2015 4th International Conference on Electric Power and Energy Conversion Systems (EPECS), Sharjah, United Arab Emirates: IEEE, nov. 2015, p. 1-5. doi: 10.1109/EPECS.2015.7368500.
- [5] P. Nielsen, F. Blaabjerg, et J. K. Pedersen, « Space vector modulated matrix converter with minimized number of switchings and a feedforward compensation of input voltage unbalance », in Proceedings of International Conference on Power Electronics, Drives and Energy Systems for Industrial Growth, New Delhi, India: IEEE, 1995, p. 833-839. doi: 10.1109/PEDES.1996.536381.
- [6] M. Chai, R. Dutta, et J. Fletcher, « Space vector PWM for three-to-five phase indirect matrix converters with d2-q2 vector elimination », in IECON 2013 - 39th Annual Conference of the

- IEEE Industrial Electronics Society, Vienna, Austria: IEEE, nov. 2013, p. 4937-4942. doi: 10.1109/IECON.2013.6699934.
- [7] K. Rahman, A. Iqbal, M. A. Al-Hitmi, O. Dordevic, et S. Ahmad, « Performance Analysis of a Three-to-Five Phase Dual Matrix Converter Based on Space Vector Pulse Width Modulation », *IEEE Access*, vol. 7, p. 12307-12318, 2019, doi: 10.1109/ACCESS.2019.2892514.
- [8] Q.-H. Tran et H.-H. Lee, « An Advanced Modulation Strategy for Three-to-Five-Phase Indirect Matrix Converters to Reduce Common-Mode Voltage With Enhanced Output Performance », *IEEE Trans. Ind. Electron.*, vol. 65, no 7, p. 5282-5291, juill. 2018, doi: 10.1109/TIE.2017.2782242.
- [9] T. D. Nguyen et H.-H. Lee, « Development of a Three-to-Five-Phase Indirect Matrix Converter With Carrier-Based PWM Based on Space-Vector Modulation Analysis », *IEEE Trans. Ind. Electron.*, vol. 63, no 1, p. 13-24, janv. 2016, doi: 10.1109/TIE.2015.2472359.
- [10] T. D. Nguyen et Hong-Hee Lee, « Carrier-based PWM technique for three-to-five phase indirect matrix converters », in *IECON 2011 - 37th Annual Conference of the IEEE Industrial Electronics Society*, Melbourne, Vic, Australia: IEEE, nov. 2011, p. 3662-3667. doi: 10.1109/IECON.2011.6119904.
- [11] S. M. Ahmed, Z. Salam, et H. Abu-Rub, « Improved Space Vector Modulation for Three-to-Seven Phase Matrix Converter with Reduced Number of Switching Vectors », *IEEE Trans. Ind. Electron.*, p. 1-1, 2014, doi: 10.1109/TIE.2014.2381158.
- [12] S. M. Dabour, S. M. Allam, et E. M. Rashad, « Indirect space-vector PWM technique for three to nine phase matrix converters », in *2015 IEEE 8th GCC Conference & Exhibition*, Muscat, Oman: IEEE, févr. 2015, p. 1-6. doi: 10.1109/IEEEGCC.2015.7060029.
- [13] G. Tozzi, M. Elsied, A. Mpanda Mabwe, C. Onambele, et L. Pugi, « Enhanced space vector PWM for six to three-phase matrix converter interfacing PMSG with the grid », in *IECON 2017 - 43rd Annual Conference of the IEEE Industrial Electronics Society*, Beijing: IEEE, oct. 2017, p. 1933-1940. doi: 10.1109/IECON.2017.8216326.
- [14] M. Mihret, M. Abreham, O. Ojo, et S. Karugaba, « Modulation schemes for five-phase to three-phase AC-AC matrix converters », in *2010 IEEE Energy Conversion Congress and Exposition*, Atlanta, GA: IEEE, sept. 2010, p. 1887-1893. doi: 10.1109/ECCE.2010.5618296.
- [15] S. M. Ahmed, H. Abu-Rub, Z. Salam, et A. Iqbal, « Space vector PWM technique for a direct five-to-three-phase matrix converter », in *IECON 2013 - 39th Annual Conference of the IEEE Industrial Electronics Society*, Vienna, Austria: IEEE, nov. 2013, p. 4943-4948. doi: 10.1109/IECON.2013.6699935.